Applied Surface Science 679 (2025) 161316

Contents lists available at ScienceDirect

Applied Surface Science

journal homepage: www.elsevier.com/locate/apsusc

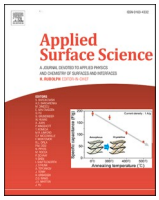

Full Length Article

# Tunneling and thermionic emission as charge transport mechanisms in W-based Schottky contacts on AlGaN/GaN heterostructures

Simone Milazzo [a,b,*], Giuseppe Greco [b], Salvatore Di Franco [b], Patrick Fiorenza [b], Filippo Giannazzo [b], Corrado Bongiorno [b], Leonardo Gervasi [c], Salvatore Mirabella [d,e], Ferdinando Iucolano [c], Fabrizio Roccaforte [b]

[a] Department of Chemical Sciences, University of Catania, Viale Andrea Doria 6, Catania 95125, Italy
[b] CNR-IMM HQ, Strada VIII, n.5 – Zona Industriale, Catania 95121, Italy
[c] STMicroelectronics, Stradale Primosole 50, Catania 95121, Italy
[d] Department of Physics and Astronomy "Ettore Majorana", University of Catania, via Santa Sofia 64, Catania 95123, Italy
[e] CNR-IMM Catania University Unit, via Santa Sofia 64, Catania 95123, Italy

ARTICLE INFO

*Keywords:*
AlGaN/GaN
Schottky contacts
Conduction mechanisms
Metal/AlGaN interface
Conductive dislocations
C-AFM

ABSTRACT

This paper investigates the forward conduction mechanism of W-based Schottky diodes on AlGaN/GaN heterostructures across a temperature range of 25–150 °C. Current-Voltage measurements carried out at different temperatures (I-V-T), allow to identify two coexisting mechanisms for charge transport. At lower bias the conduction mechanism is ruled by tunneling (TU), with a characteristic energy of $E_{00} = 75$ meV extracted from the temperature dependence of the ideality factor. At higher bias the Thermionic Emission (TE) mechanism dominates, thus revealing the presence of an inhomogeneous barrier that increases from 0.77 to 0.94 eV with increasing the measurement temperature. An ideal barrier of 1.22 eV was extrapolated for a unitary ideality factor. Structural and electrical analyses performed at nanoscale level revealed the presence of a density of defects (dislocations) in the order of $4 \times 10^9$ cm$^{-2}$. Conductive Atomic Force Microscopy (C-AFM) provided local electrical information, uncovering a significant correlation between the observed electrical characteristics and the nanoscale defect distribution. This detailed insight highlights the crucial role of the electrical characteristics of defects in influencing the tunneling current component at low bias, thereby providing valuable context for understanding the electrical behavior and performance of microscopic devices.

## 1. Introduction

Gallium nitride (GaN) is considered to be a suitable material for high-power technology, thanks to its large bandgap (3.4 eV) and high critical breakdown electric field (3.3 MV/cm) [1]. Furthermore, the fabrication of AlGaN/GaN heterostructures, due to the coexistence of spontaneous and piezoelectric polarization [2], is accompanied by a quantum confinement of negative charge defined as two-dimensional electron gas (2DEG) and characterized by a high electron mobility of about 2000 cm$^2$V$^{-1}$s$^{-1}$ [3]. For these reasons, high electron mobility transistors (HEMT) based on AlGaN/GaN heterostructures are attractive devices for the next generation of high-frequency applications.

The gate contact plays a significant role in HEMT devices, controlling the amount of charge of the 2DEG, i.e. the current flow in the channel and the overall electrical behaviour of the device [4].

In forward bias, for low doping concentrations or unintentionally doped semiconductors, the current passing through an ideal rectifying contact is rationalized by the Thermionic Emission (TE) model. The forward current depends on the applied voltage on the contact and the energetic value of the Schottky Barrier Height (SBH). The SBH is crucial in diodes and HEMTs, since it affects many parameters such as the reverse bias leakage [5], the turn-on voltage [6], the threshold voltage [7], or the subthreshold swing [8]. In this context, the investigation of the conduction mechanism at the metal/semiconductor interface is of paramount importance when considering the reliability of the devices. In fact, a high gate current can have several adverse effects, such as undesired threshold voltage swings due to the charging of trap states under the gate contact [7] and in general reliability problems due to power dissipation and reduced lifetime [9].

According to the TE model, ideal Schottky contacts do not

* Corresponding author at: CNR-IMM HQ, Strada VIII, n.5 – Zona Industriale, Catania 95121, Italy.
*E-mail address:* simone.milazzo@imm.cnr.it (S. Milazzo).

https://doi.org/10.1016/j.apsusc.2024.161316
Received 10 June 2024; Received in revised form 13 September 2024; Accepted 22 September 2024
Available online 23 September 2024

contemplate a temperature dependence of the ideality factor, and its value should remain constant and close to unity. In AlGaN/GaN heterostructures the TE model is generally invoked to explain the forward conduction mechanism, but a high value of the ideality factor (>2) and its temperature dependence are typically found. Indeed, the ideality factor decreases while the SBH slightly increases with temperature. When the ideality factor and the SBH show a temperature dependence, this behavior is often ascribed to the barrier inhomogeneity or the presence of defects in the semiconductor [10]. Although the TE model is often employed in the description of the conduction mechanism at the metal/semiconductor interface, strong deviations from the ideal behaviour are frequently observed and other mechanisms must be taken into account. In this context, the dominance of one charge-transport mechanism over another depends on a variety of factors ranging from sample preparation [11,12] to material quality as on the presence of structural defects. Other mechanisms such as Thermionic Field Emission (TFE) have been observed in recessed devices [13]. In such geometry, the Schottky barrier becomes thinner due to the direct contact at the edge of the recessed Schottky metal with the GaN surface, which has a high density of charge due to the 2DEG.

Some authors have shown, both on Silicon Carbide [14] and Gallium Nitride [15], that the temperature dependence of the SBH and ideality factor suggests the presence of an inhomogeneous barrier at the metal/semiconductor interface which contributes in forming preferential conduction paths in some regions of the contact, reducing the effective area of the Schottky contact.

In previous studies C-AFM has been used to study the effect of structural defects on the behaviour of AlGaN/GaN transistors. C-AFM measurements conducted on top of the AlGaN surface have highlighted an inhomogeneous conduction at the Tip/AlGaN interface [16].

On AlGaN/GaN heterostructures, anomalous I-V characteristics have been rationalized employing the “two diodes model” [17]. The deviations from the ideal TE behavior are explained considering the presence of metal/AlGaN/GaN system as composed of two “back-to-back” diodes, the first one (metal/AlGaN) being forward biased while the second one (AlGaN/GaN) reverse biased. This approach considers the presence of two Schottky barriers, and allowed for the extraction of a value of the Schottky Barrier Height coherent with the Schottky-Mott relation.

Also, the description of the conduction mechanisms involving heterostructures such as AlGaN/GaN is based on the hypothesis that there are many concurrent mechanisms, where the tunneling phenomenon is generally considered as the dominant contributor to the measured current [18].

Arslan et al. [19] have rationalized the transport mechanism in Ni/Au Schottky contacts in AlGaN/GaN heterostructures and ascribed the experimental electrical behaviour to multiple mechanisms in a temperature range from 80 to 410 K. The presence of threading dislocations ($0.24 \times 10^7$ $cm^{-2}$, measured by XRD analysis) is the main factor that makes the tunneling conduction mechanism to be the dominant one.

A similar behaviour has been observed also by Donoval et al. [20] in Ni-based Schottky diodes on InAlN/GaN heterostructures. Also in this case the J-V curve is fitted in a temperature range from 300 to 600 K and the experimental current density is predominantly due to a tunneling conduction.

Yan et al. [21] have attested that the TE model alone fails to describe the conduction mechanism at the interface of Ni/Au-AlGaN/GaN Schottky diodes, explaining the conduction mechanism as the results of tunneling and thermionic emission mechanisms. The experimental I-V curve fits with the tunneling model over a wide bias range, while the thermionic emission model only slightly prevails over the tunneling model at higher temperatures for high bias.

The relationship between defect density and both electrical and optical properties is significant [22]. Traditional methods for the estimation of the dislocation density are TEM and XRD analyses but they are inadequate for assessing the electrical properties crucial for electronic devices. To complement structural analyses, electrical-sensitive techniques, such as Hall measurements [23] are employed. For detailed studies, C-AFM stands out as another technique characterized by high spatial resolution and direct electrical characterization. C-AFM has enabled a detailed study of the electronic distribution around a threading edge dislocation in n-GaN films [24] revealing the presence of acceptor states near the valance band near this kind of dislocations. Additionally, threading screw dislocations have been found to be electrically neutral in n-GaN [25] but they contribute to the formation of pipes [22].

C-AFM techniques provide a direct and localized assessment of the electrical properties of the surface of the material, making it a valuable tool for understanding the electrical behavior of defects in semiconductor materials and their impact on devices’ performances.

In this paper the forward conduction mechanism of W-based Schottky Barrier Diodes (SBDs) fabricated on AlGaN/GaN heterostructures has been characterized. The electrical measurements performed at different temperatures allowed for the rationalization of the conduction behavior of the diodes. Two distinct mechanisms, namely TE and tunneling, have been employed. Tunneling predominantly contributes to the total conduction mechanism at room temperature, particularly at low bias (<0.75 V). Thermionic Emission plays a more significant role at higher bias. The bias at which the two mechanisms have the same strength has been defined as “Overlap Bias”, with a marked dependence on the temperature. In order to get an insight into the origin of the tunneling contribution, nanoscale analysis have been conducted, such as conductive atomic force microscopy (C-AFM) and scanning transmission electron microscopy (STEM).

## 2. Experimental

AlGaN/GaN heterostructures grown on Si substrates have been used in this work. The AlGaN barrier layer had a thickness of 16 nm and Al concentration of 26 %. On this heterostructure, lateral Schottky diodes have been fabricated having Ta-based metal as ohmic contacts [26]. Schottky contacts are composed of a W-based metal to ensure Au-free contacts and to achieve moderate values of barrier height. The diodes consisted of a circular Schottky anode of variable diameter (100, 200 and 400 μm), surrounded by a large area ohmic contact. The devices have been characterized by electrical measurements (I-V-T) to get an insight into the Schottky contact properties. Thermal electrical measurements have been acquired in a Karl-Suss Microtech probe station equipped with a parameter analyser for I-V-T analysis, the explored thermal range is 25 to 150 °C.

Also nanoscale analyses have been conducted to estimate the concentration of defects and their contribution to the conduction mechanism. Scanning Transmission Electron Microscopy (STEM) analyses on a reference AlGaN/GaN heterostructure were performed with JEOL ARM200C at 200 keV. The current transport on the semiconductor surface was investigated at the nanoscale by performing conductive-atomic force microscopy (C-AFM) current mapping characterizations with diamond-coated Si tips, using DI 3100 AFM equipment (Bruker, San Francisco, CA, USA) with Nanoscope V electronics.

## 3. Results and discussion

Fig. 1 shows the semi-logarithmic plot of the forward current density–voltage (J-V) characteristics of the Schottky diodes, measured at various temperatures from 25 to 150 °C. The J-V curves display a non ideal-behavior, characterized by a distinctive pattern. Initially, as the bias increases, the current density grows exponentially, defined as Region I. However, at a certain bias point, the curves bend downwards. This bend is less pronounced at higher temperatures. Following this transition, the current density resumes to grow exponentially, defined as Region II, and finally reaches the saturation level. The current at a larger applied bias than 1.5 V is only slightly decreasing with temperature, due

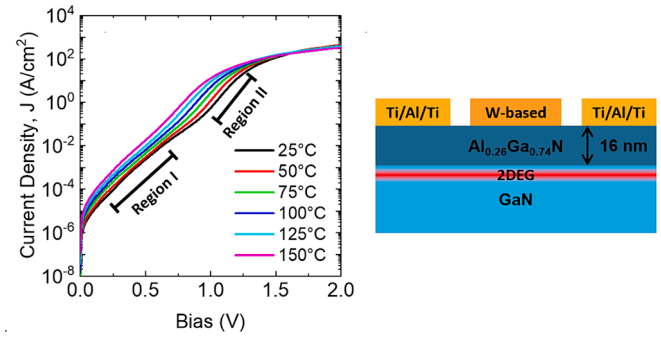


**Fig. 1.** Forward J-V characteristics of the W-based/AlGaN/GaN Schottky diodes at different temperatures and schematic diagram of the investigated SBDs.

to the series resistance contribution that limits the overall conduction of the measured device.

This bending in the J-V curves occurs at a different bias values depending on the temperature and allows to distinguish two linear regions, namely Region I at low bias and Region II at high bias. The higher the measurement temperature and the lower will be the bias value at which there's the transition between the two regions.

Indeed, Region II can be described by TE theory, according to which the forward current has the following expression

$$J_F = J_S \exp\left(\frac{qV_F}{nkT}\right) = A^* T^2 \exp\left(-\frac{q\Phi_B}{k_B T}\right)\exp\left(\frac{qV_F}{nk_B T}\right) \quad (1)$$

where A* is the Richardson constant (32 A $cm^{-2}$ $K^{-2}$) [4], T is the absolute temperature, q is the elementary charge, $k_B$ is the Boltzmann constant, $\Phi_B$ is the Schottky Barrier Height, and n is the ideality factor.

By performing a linear fit in Region II, it was possible to extract SBH and n for each temperature. Fig. 2a shows the thermal behaviour of the extracted SBH and n. In particular, it can be noticed that from 25 to 150 °C the SBH increases from 0.77 to 0.93 eV, while n decreases from 2.59 to 1.97. This behaviour is typically observed in inhomogeneous barrier [10].

By plotting the SBH as a function of the ideality factor (Fig. 2b), a linear correlation between these two parameters is found, from which it was possible to extract the value of $\Phi_B^0 = 1.22$ eV for an ideality factor of unitary value. The value of $\Phi_B^0$ can be seen as the value of the barrier height expected for a homogenous SBH [10,14,15,27].

To show the inadequacy of the TE model at low bias, the same approach has been employed in Region I. In this case, the ideality factor reaches well higher values, up to 2.9 at room temperature. Indeed, the thermal behavior of n clearly points out the inadequacy of the assumption of a TE mechanism for this bias region. Fig. 3 reports the experimental values of the ideality factor extracted by fitting, in the two linear regions, the J-V curves in a $nk_BT/k_BT$ plot. The plot includes also the unitary value of the ideality factor to represent ideal TE behavior. As

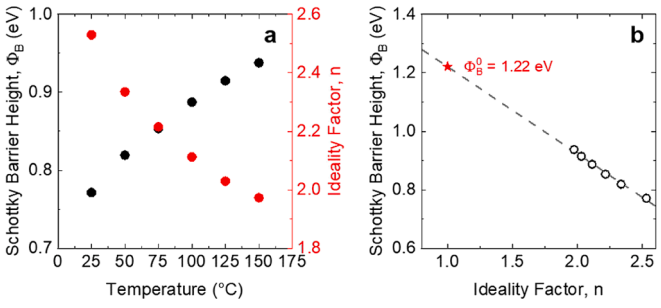


**Fig. 2.** SBH and n of W-based/AlGaN/GaN Schottky diodes extracted with the TE model applied in Region II at different temperatures (a), and SBH/n plot with an ideal SBH of 1.22 eV.

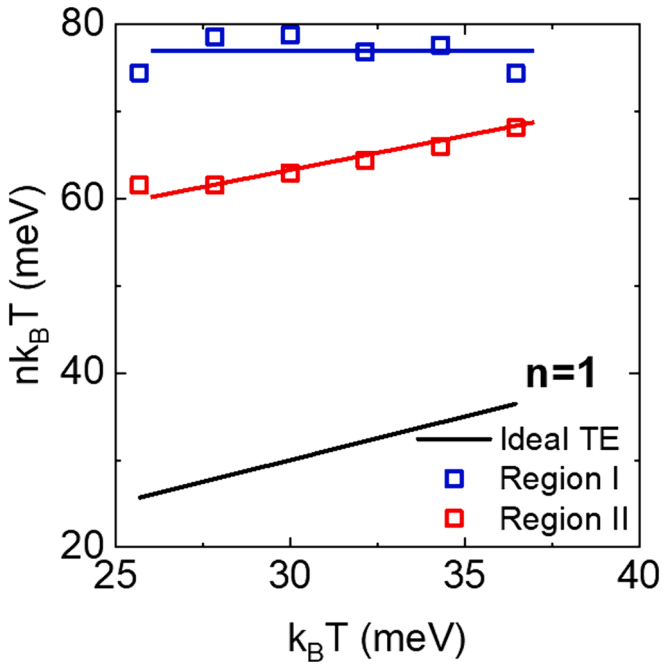


**Fig. 3.** Experimental values of $nk_BT$ versus $k_BT$ extracted in the two regions of the J-V curves (empty simbols) and theoretical value for ideal Thermionic Emission (black line).

can be seen, the ideal case (solid black line) shows a linear increase of $nk_BT$ with temperature. This behavior is also shown by Region II (red symbols). Here there's the same trend but shifted upwards which is associated with high experimental values of ideality factors. In this bias range the conduction mechanism is dominated by thermionic emission. Meanwhile in Region I (blue symbols) almost thermally insensitive values of $nk_BT$ are extracted, this behavior is symptomatic of a conduction mechanism dominated by tunneling [10,28,29]. So, the electrical behavior observed in Region I will be better described by a tunneling model rather than the thermionic emission model.

According to tunneling model, the current density can be expressed as

$$J_F = J_0 \exp\left(\frac{qV_F}{E_0}\right) \quad (2)$$

where $J_0$ is the saturation value of the tunneling current density and $E_0$ is the "tunneling parameter", somehow similar to the ideality factor in the TE model. $E_0$ can be thought as the energy at which there is a maximum in tunneling probability through a barrier [30], expressed as

$$E_0 = E_{00}\coth\left(\frac{E_{00}}{k_B T}\right) \quad (3)$$

with $E_{00}$ defined as characteristic tunneling energy related to the tunnel effect transmission probability [20].

Moreover, the tunneling parameter $E_0$ can be correlated with the ideality factor of the TE model, according the equation [4,19].

$$E_0 = nk_BT \quad (4)$$

Once the ideality factor has been extracted for each measurement temperature in Region I, the value of $E_{00}$ that best fits with experimental data can be found, according to Equation (3) and Equation (4). Indeed, in Fig. 4, the ideality factor is plotted as a function of temperature, together with the theoretical values of the ideality factors calculated for different $E_{00}$ values (from 50 meV to 80 meV). The ideality factor values increase with increasing characteristic tunneling energy $E_{00}$ and also they are characterized by a more pronounced thermal sensitivity. On the other hand, if the characteristic tunneling energy $E_{00}$ decreases, the

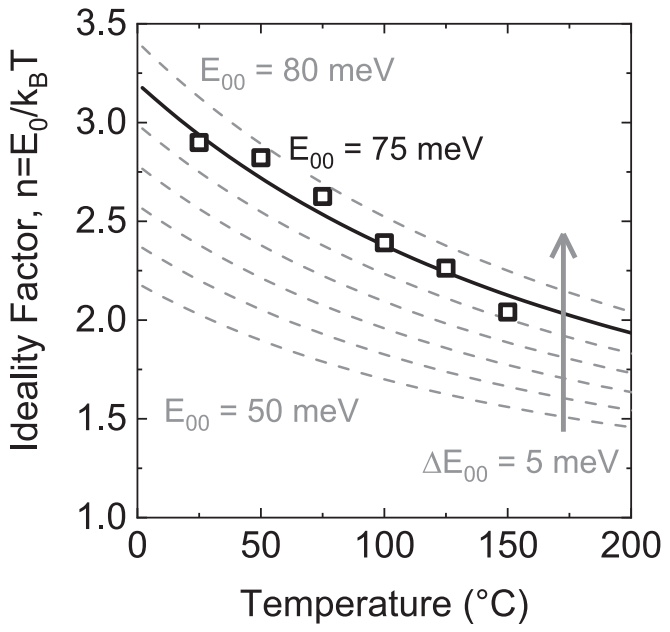


**Fig. 4.** Temperature dependence of the ideality factor extracted in Region I of W-based/AlGaN/GaN Schottky diodes.

ideality factors approach a unitary value and are characterized by a weaker sensitivity to temperature, approaching the TE model. From the fit of the experimental data a characteristic tunneling energy $E_{00} = 75$ meV has been estimated. Previously reported values of $E_{00}$ on AlGaN/GaN heterostructures range from 25 to 85 meV [4,19,20].

Once the tunneling parameter ($E_0$), the Schottky Barrier Height (SBH) and ideality factor (n) have been obtained for each measurement temperature, considering respectively tunneling and thermionic emission mechanisms, it was possible to rationalize the overall conduction mechanisms of the fabricated W-based Schottky diodes. In Fig. 5 the J-V curves and the corresponding fit performed with the TU model (blue lines) and TE model (red lines) are displayed at 25 °C (Fig. 5a) and 150 °C (Fig. 5b). At 25 °C, Fig. 5a, the two modelled current densities intersect each other at 0.9 V. The bias value associated to this intersection has been defined as the "Overlap Bias". For any temperature measurement, the Overlap Bias defines the bias value for which one mechanism prevails over the other. When the applied bias is lower than the Overlap Bias the major contribution to the total current density is due to the tunneling conduction, while at higher applied bias the largest contribution is due to thermionic emission. When temperature is raised from 25 °C to 150 °C, a shift of the Overlap Bias towards lower bias is observed, Fig. 5c, thus meaning that TE becomes the major contributor to the total current density even at lower bias levels.

In the previously mentioned works [19–21], the increase in temperature does not have an impactful consequence on the models employed to explain the experimental current density, meaning that the conduction by tunneling is the most predominant mechanism over a wide range of applied bias. For the investigated W-based/AlGaN/GaN Schottky diodes reported in this paper, Thermionic Emission has a highest weight over the Tunneling at high bias, but also increases its contribution at low bias with increasing the temperature.

The series resistance ($R_S$) has been determined by fitting the experimental data to the equations representing the two detected mechanisms (from Equation (1) for TE, and Equation (2) for TU). The $R_S$ value contribute to reduce the real applied bias to $V_F$-$J_F R_S$. The different values of the obtained $R_S$ in the two linear regions (i.e. corresponding to the two mechanisms) are attributed to different area percentage that contributes to the total current for each mechanism. Through this fitting procedure, series resistance values for each transport mechanism within the metal/semiconductor interface have been extracted. The results show that thermionic emission is the dominant mechanism, contributing 99.8 % to the total resistance of the contact area. However, despite its minor contribution of 0.2 %, the consideration of the tunnel effect and the study of the underlying causes are crucial for a comprehensive and robust modeling of the system.

The tunneling model used in this paper predicts a conduction that is governed by multistep tunneling with the involvement of dislocations [31–33]. The saturation current can be analytically described as

$$I_0 = qD\nu_D \exp\left(-\frac{\Phi_B - \mu_n}{E_0}\right) \quad (5)$$

Where q is the fundamental charge, D is the dislocation density, $\nu_D$ is the Debye frequency ($1.68 \times 10^{13}$ $s^{-1}$) [19], $\Phi_B$ is the Schottky Barrier Height, $\mu_n$ is the chemical potential and $E_0$ is the tunneling parameter.

From this equation, known the saturation tunneling current extracted from the linear fits in Region I of the I-V curves, and the value of the tunneling parameter for each measurement temperature, it's possible to extract a value of dislocation density equal to $9 \times 10^8$ $cm^{-2}$.

To clarify the origin of the tunneling contribution to the measured current density, nanoscale analysis have been conducted. In particular AFM and C-AFM analyses have been performed on the bare surface of AlGaN/GaN heterostructures to get an insight on the material quality. In Fig. 6a the morphological AFM image in tapping mode shows the presence of grain boundaries and also topological depressions. These lower regions in the morphology image are present both along the crystal domain and also inside each crystal domain. These pits are commonly associated to defects that occur during the deposition of the material and are present on top of screw dislocations [34]. The C-AFM

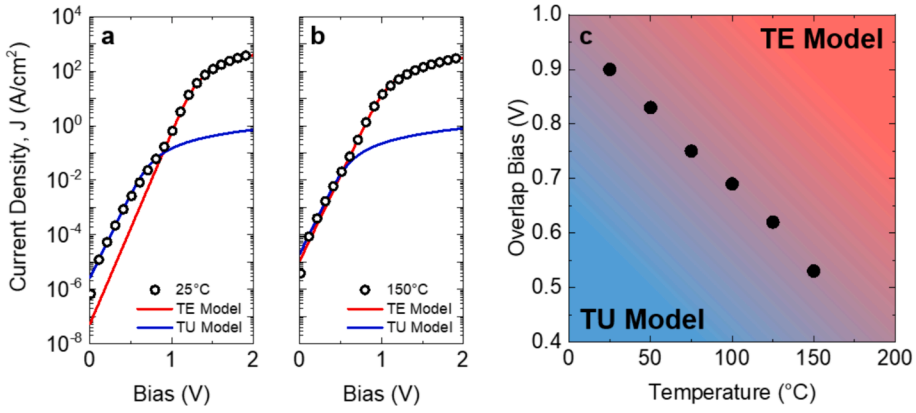


**Fig. 5.** J-V curves measured at 25 °C (a) and 150 °C (b) and fittings according to TE model (red lines) and TU model (blue lines), and the thermal dependence of the Overlap Bias (c).

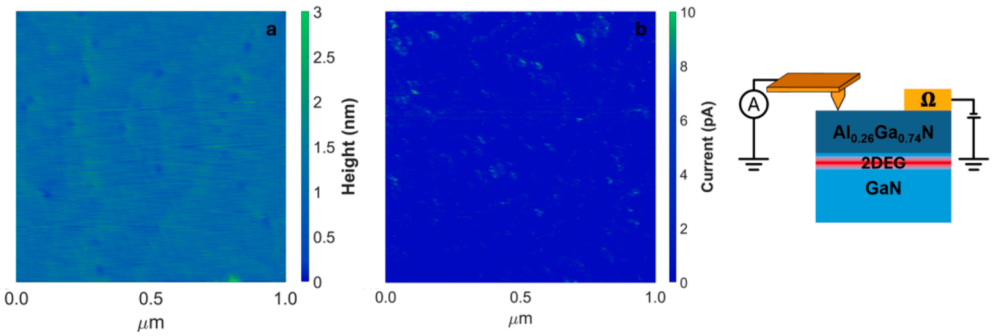


**Fig. 6.** Morphological AFM image in tapping mode (a) and current image (b) of the AlGaN/GaN heterostructure, schematic of the experimental setup for C-AFM analyses.

image, Fig. 6b, has been conducted in lateral conditions by applying a DC bias of 1.6 V, and it gives an insight in the uniformity of electrical conduction of the scanned area. The current map exhibits an inhomogeneous current distribution characterized by regions with high measured current in a backdrop of lower current. These highly conductive areas account for 0.2 % of the scanned area.

Moreover, STEM analyses were performed to examine the structural quality of the material and presence of possible defects which could justify such electrical behavior. In Fig. 7 the in-plane STEM of the AlGaN/GaN heterostructure is displayed. According to the tapping AFM morphological image, it's possible to see the presence of grain boundaries characterized by a high concentration of dislocations around the junction between different crystal domains. Additionally, within each crystalline domain, further dislocations are discerned. The cumulative dislocation density is measured to be $4 \times 10^9$ cm$^{-2}$. Concerning AlGaN/GaN heterostructures grown by MOCVD, the dislocation density oscillates around 1–5 $\times$ $10^9$ cm$^{-2}$ both for AlGaN/GaN heterostructures grown on silicon [35] and other substrates like sapphire [36].

Interestingly, from the electrical analyses on the macroscopic diodes it has been possible to quantify the area contribution of each mechanism. The Tunneling mechanism contributes by 0.2 % of the total area while the Thermionic Emission mechanism for the remaining 99.8 %. This finding has a direct correlation with the nanoscale analyses that indicate a high concentration of defects, such as dislocation, that generate an inhomogeneous current conduction at one bias level. The C-AFM image (Fig. 6b) shows high conduction regions associated to 0.2 % of the total scanned area, coherently with what is observed from the electrical measurements. Also according to the tunneling model used, it's possible to estimate analytically a dislocation concentration of 9 $\times$ $10^8$ cm$^{-2}$. The difference between the value estimated through STEM analysis ($4 \times 10^9$ cm$^{-2}$) and the one predicted by the model could be associated to the different electrical behavior of dislocations [37], generally threading dislocations are the one that contribute more to the electrical conduction [37,38].

The characterization of the W-based SBDs allows for the depiction of a possible band diagram in Fig. 8. Particularly, the contact is inhomogeneous, meaning that along the lateral coordinate of the contact the punctual value of the SBH is different along an average value. Also, from the electrical characterization the conclusion that there are two mechanisms present can be drawn, involving both Thermionic Emission and Tunneling. Where the Tunneling mechanism (blue arrow) can be attributed to the presence of dislocations, so that the charge in forward bias tunnels across the AlGaN barrier with the aid of defects inside the material (red cylinders). Meanwhile according to the Thermionic Emission mechanism (red arrow) the charge overcomes the barrier. Depending on the bias value applied to the Schottky contact the relative weight of the two mechanisms changes, referred as Region I where the TU prevails, while Region II where the TE prevails (Fig. 1).

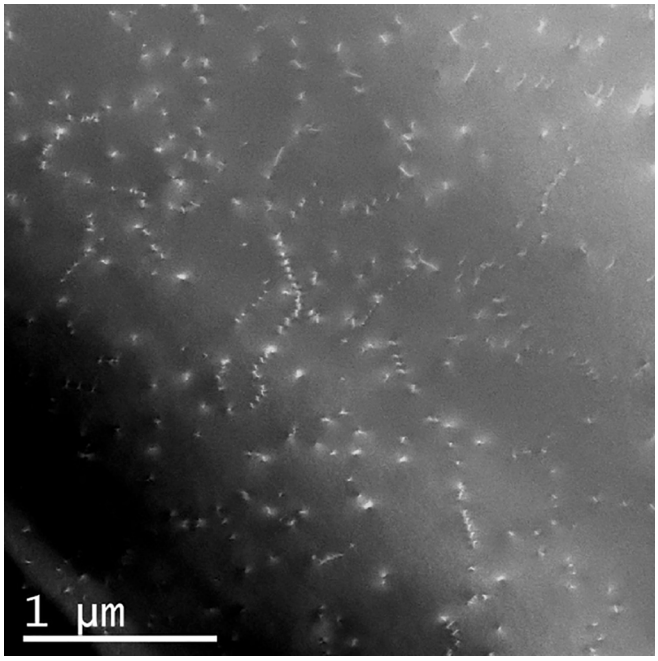


**Fig. 7.** In-plane STEM image of the AlGaN/GaN heterostructure.

## 4. Conclusion

This study provides an in-depth analysis of W-based Schottky diodes fabricated on AlGaN/GaN heterostructures, employing a multi-faceted approach to investigate their electrical behavior across a temperature range of 25 °C to 150 °C. Through I-V-T measurements, two conduction

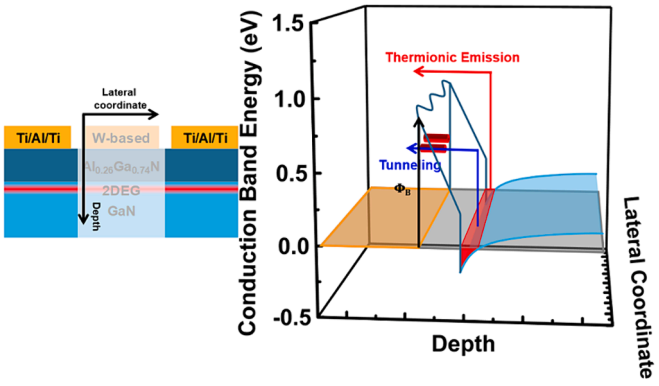


**Fig. 8.** Sketch of a three-dimensional Conduction Band Energy Diagram of the investigated W-based/AlGaN/GaN SBDs.

models, Thermionic Emission and Tunneling, allow for the complete explanation of the overall conduction mechanism. By studying the thermal dependence of the ideality factor in the region where tunneling prevails over the thermionic emission, a characteristic tunneling energy ($E_{00}$) of 75 meV was extracted. The series resistance analysis revealed that only 0.2 % of the contact area contributes to tunneling, while in the remaining 99.8 % is thermionic emission. Moreover, the concept of the Overlap Bias was introduced, representing the bias value at which one conduction mechanism prevails over the other. It was observed that the Overlap Bias shifted towards lower bias with increasing temperature, indicating a transition from tunneling-dominated conduction to thermionic emission-dominated conduction. This thermal dependence of the Overlap Bias provides valuable insights into the dynamic interplay between conduction mechanisms and temperature variations in the Schottky diodes. Nanoscale analyses provided further understanding of the factors influencing the tunneling contribution to the conduction mechanism. STEM analysis revealed a dislocation density of $4 \times 10^9$ $cm^{-2}$, indicating the presence of structural defects affecting device performance. C-AFM further underscored this by revealing inhomogeneities in current density, identifying current hot spots corresponding to 0.2 % of the total area. The integration of I-V-T measurements conducted on diodes with nanoscale analyses (C-AFM) consistently demonstrated that 0.2 % of the conduction occurs via tunneling facilitated by dislocations. These findings illuminate the complex relationships between device properties, material defects, and conduction mechanisms in W-based Schottky diodes, showcasing the value of a multi-technique approach in achieving a comprehensive understanding of device behavior.

## CRediT authorship contribution statement

**Simone Milazzo:** Writing – review & editing, Writing – original draft, Investigation, Formal analysis, Data curation. **Giuseppe Greco:** Writing – review & editing, Supervision, Methodology, Data curation, Conceptualization. **Salvatore Di Franco:** Validation, Supervision. **Patrick Fiorenza:** Validation, Methodology, Investigation. **Filippo Giannazzo:** Validation, Methodology, Investigation. **Corrado Bongiorno:** Methodology, Investigation. **Leonardo Gervasi:** Validation. **Salvatore Mirabella:** Writing – review & editing, Validation, Supervision. **Ferdinando Iucolano:** Visualization, Validation. **Fabrizio Roccaforte:** Writing – review & editing, Validation, Supervision, Project administration, Methodology, Investigation, Conceptualization.

## Declaration of competing interest

The authors declare that they have no known competing financial interests or personal relationships that could have appeared to influence the work reported in this paper.

## Data availability

Data will be made available on request.

## Acknowledgements

This work was supported by the European Union (NextGeneration EU), through the MUR-PNRR projects SAMOTHRACE (Nos. PNRRM4C2 and ECS00000022).

## References

[1] F. Roccaforte, P. Fiorenza, R. Lo Nigro, F. Giannazzo, G. Greco, Physics and technology of gallium nitride materials for power electronics, Riv. Nuovo Cimento 41 (2018) 625–681, https://doi.org/10.1393/ncr/i2018-10154-x.
[2] J.P. Ibbetson, P.T. Fini, K.D. Ness, S.P. DenBaars, J.S. Speck, U.K. Mishra, Polarization effects, surface states, and the source of electrons in AlGaN/GaN heterostructure field effect transistors, Appl. Phys. Lett. 77 (2000) 250–252, https://doi.org/10.1063/1.126940.
[3] O. Ambacher, B. Foutz, J. Smart, J.R. Shealy, N.G. Weimann, K. Chu, M. Murphy, A.J. Sierakowski, W.J. Schaff, L.F. Eastman, R. Dimitrov, A. Mitchell, M. Stutzmann, Two dimensional electron gases induced by spontaneous and piezoelectric polarization in undoped and doped AlGaN/GaN heterostructures, J. Appl. Phys. 87 (2000) 334–344, https://doi.org/10.1063/1.371866.
[4] G. Greco, P. Fiorenza, M. Spera, F. Giannazzo, F. Roccaforte, Forward and reverse current transport mechanisms in tungsten carbide Schottky contacts on AlGaN/GaN heterostructures, J. Appl. Phys. 129 (2021) 234501, https://doi.org/10.1063/5.0052079.
[5] H. Hasegawa, S. Oyama, Mechanism of anomalous current transport in n -type GaN Schottky contacts, J. Vacuum Sci. Technol. B: Microelectr. Nanometer Struct. Process. Meas. Phenomena 20 (2002) 1647–1655, https://doi.org/10.1116/1.1491539.
[6] T. Zhang, J. Zhang, W. Zhang, Y. Zhang, X. Duan, J. Ning, Y. Hao, Investigation of an AlGaN-channel Schottky barrier diode on a silicon substrate with a molybdenum anode, Semicond. Sci. Technol. 36 (2021) 044003, https://doi.org/10.1088/1361-6641/abcbd5.
[7] G. Meneghesso, M. Meneghini, D. Bisi, I. Rossetto, A. Cester, U.K. Mishra, E. Zanoni, Trapping phenomena in AlGaN/GaN HEMTs: a study based on pulsed and transient measurements, Semicond. Sci. Technol. 28 (2013) 074021, https://doi.org/10.1088/0268-1242/28/7/074021.
[8] J.W. Chung, J.C. Roberts, E.L. Piner, T. Palacios, Effect of Gate Leakage in the Subthreshold Characteristics of AlGaN/GaN HEMTs, IEEE Electron Device Lett. 29 (2008) 1196–1198, https://doi.org/10.1109/LED.2008.2005257.
[9] R. Trew, D. Green, J. Shealy, AlGaN/GaN HFET reliability, IEEE Microwave 10 (2009) 116–127, https://doi.org/10.1109/MMM.2009.932286.
[10] R.T. Tung, Electron transport at metal-semiconductor interfaces: General theory, Phys. Rev. B 45 (1992) 13509–13523, https://doi.org/10.1103/PhysRevB.45.13509.
[11] H. Hasegawa, T. Inagaki, S. Ootomo, T. Hashizume, Mechanisms of current collapse and gate leakage currents in AlGaN/GaN heterostructure field effect transistors, J. Vacuum Sci. Technol. B: Microelectr. Nanometer Struct. Process. Meas. Phenomena 21 (2003) 1844–1855, https://doi.org/10.1116/1.1589520.
[12] H. Hasegawa, M. Akazawa, Steady state and transient behavior of currents in AlGaN/GaN planar Schottky diodes and mechanism of current collapse, J. Vacuum Sci. Technol. B: Microelectr. Nanometer Struct. Process. Meas. Phenomena 26 (2008) 1542–1550, https://doi.org/10.1116/1.2929865.
[13] Y. Yao, J. Zhong, Y. Zheng, F. Yang, Y. Ni, Z. He, Z. Shen, G. Zhou, S. Wang, J. Zhang, J. Li, D. Zhou, Z. Wu, B. Zhang, Y. Liu, Current transport mechanism of AlGaN/GaN Schottky barrier diode with fully recessed Schottky anode, Jpn. J. Appl. Phys. 54 (2015) 011001, https://doi.org/10.7567/JJAP.54.011001.
[14] F. Roccaforte, F. La Via, V. Raineri, R. Pierobon, E. Zanoni, Richardson's constant in inhomogeneous silicon carbide Schottky contacts, J. Appl. Phys. 93 (2003) 9137–9144, https://doi.org/10.1063/1.1573750.
[15] F. Iucolano, F. Roccaforte, F. Giannazzo, V. Raineri, Barrier inhomogeneity and electrical properties of Pt/GaN Schottky contacts, J. Appl. Phys. 102 (2007) 113701, https://doi.org/10.1063/1.2817647.
[16] A. Fontserè, A. Pérez-Tomás, M. Placidi, J. Llobet, N. Baron, S. Chenot, Y. Cordier, J.C. Moreno, M.R. Jennings, P.M. Gammon, C.A. Fisher, V. Iglesias, M. Porti, A. Bayerl, M. Lanza, M. Nafría, Nanoscale investigation of AlGaN/GaN-on-Si high electron mobility transistors, Nanotechnology 23 (2012) 395204, https://doi.org/10.1088/0957-4484/23/39/395204.
[17] G. Greco, F. Giannazzo, F. Roccaforte, Temperature dependent forward current-voltage characteristics of Ni/Au Schottky contacts on AlGaN/GaN heterostructures described by a two diodes model, J. Appl. Phys. 121 (2017) 045701, https://doi.org/10.1063/1.4974868.
[18] H. Kim, S. Choi, B.J. Choi, Forward Current Transport Properties of AlGaN/GaN Schottky Diodes Prepared by Atomic Layer Deposition, Coatings 10 (2020) 194, https://doi.org/10.3390/coatings10020194.
[19] E. Arslan, Ş. Altındal, S. Özçelik, E. Ozbay, Dislocation-governed current-transport mechanism in (Ni/Au)–AlGaN/AlN/GaN heterostructures, J. Appl. Phys. 105 (2009) 023705, https://doi.org/10.1063/1.3068202.
[20] D. Donoval, A. Chvála, R. Šramatý, J. Kováč, J.-F. Carlin, N. Grandjean, G. Pozzovivo, J. Kuzmík, D. Pogany, G. Strasser, P. Kordoš, Current transport and barrier height evaluation in Ni/InAlN/GaN Schottky diodes, Appl. Phys. Lett. 96 (2010) 223501, https://doi.org/10.1063/1.3442486.
[21] D. Yan, J. Jiao, J. Ren, G. Yang, X. Gu, Forward current transport mechanisms in Ni/Au-AlGaN/GaN Schottky diodes, J. Appl. Phys. 114 (2013) 144511, https://doi.org/10.1063/1.4824296.
[22] J.H. You, H.T. Johnson, Chapter 3 Effect of Dislocations on Electrical and Optical Properties in GaAs and GaN, in: Solid State Physics, Elsevier, 2009: pp. 143–261. https://doi.org/10.1016/S0081-1947(09)00003-4.
[23] N.G. Weimann, L.F. Eastman, D. Doppalapudi, H.M. Ng, T.D. Moustakas, Scattering of electrons at threading dislocations in GaN, J. Appl. Phys. 83 (1998) 3656–3659, https://doi.org/10.1063/1.366585.
[24] P.J. Hansen, Y.E. Strausser, A.N. Erickson, E.J. Tarsa, P. Kozodoy, E.G. Brazel, J. P. Ibbetson, U. Mishra, V. Narayanamurti, S.P. DenBaars, J.S. Speck, Scanning capacitance microscopy imaging of threading dislocations in GaN films grown on (0001) sapphire by metalorganic chemical vapor deposition, Appl. Phys. Lett. 72 (1998) 2247–2249, https://doi.org/10.1063/1.121268.
[25] X.G. Qiu, Y. Segawa, Q.K. Xue, Q.Z. Xue, T. Sakurai, Influence of threading dislocations on the near-bandedge photoluminescence of wurtzite GaN thin films on SiC substrate, Appl. Phys. Lett. 77 (2000) 1316–1318, https://doi.org/10.1063/1.1289911.

[26] G. Greco, S. Di Franco, R. Lo Nigro, C. Bongiorno, M. Spera, P. Badalà, F. Iucolano, F. Roccaforte, Improvement of Ti/Al/Ti Ohmic contacts on AlGaN/GaN heterostructures by insertion of a thin carbon interfacial layer, Appl. Phys. Lett. 124 (2024) 012103, https://doi.org/10.1063/5.0180862.
[27] H.H. Gullu, D. Seme Sirin, D.E. Yıldız, Analysis of Double Gaussian Distribution on Barrier Inhomogeneity in a Au/n-4H SiC Schottky Diode, J. Electron. Mater. 50 (2021) 7044–7056, https://doi.org/10.1007/s11664-021-09254-3.
[28] E. Arslan, Ş. Altındal, S. Özçelik, E. Ozbay, Tunneling current via dislocations in Schottky diodes on AlInN/AlN/GaN heterostructures, Semicond. Sci. Technol. 24 (2009) 075003, https://doi.org/10.1088/0268-1242/24/7/075003.
[29] M. Wu, D.-Y. Zheng, Y. Wang, W.-W. Chen, K. Zhang, X.-H. Ma, J.-C. Zhang, Y. Hao, Schottky forward current transport mechanisms in AlGaN/GaN HEMTs over a wide temperature range, Chinese Phys. B 23 (2014) 097307, https://doi.org/10.1088/1674-1056/23/9/097307.
[30] S.M. Sze, K.K. Ng, Physics of semiconductor devices, 3rd ed, Wiley-Interscience, Hoboken, N.J., 2007.
[31] V.V. Evstropov, Y.V. Zhilyaev, M. Dzhumaeva, N. Nazarov, Tunnel excess current in nondegenerate barrier (p-n and m-s) silicon-containing III–V structures, Semiconductors 31 (1997) 115–120, https://doi.org/10.1134/1.1187092.
[32] V.V. Evstropov, M. Dzhumaeva, Y.V. Zhilyaev, N. Nazarov, A.A. Sitnikova, L. M. Fedorov, The dislocation origin and model of excess tunnel current in GaP p-n structures, Semiconductors 34 (2000) 1305–1310, https://doi.org/10.1134/1.1325428.
[33] A.E. Belyaev, N.S. Boltovets, V.N. Ivanov, V.P. Klad'ko, R.V. Konakova, Ya.Ya. Kudrik, A.V. Kuchuk, V.V. Milenin, Yu.N. Sveshnikov, V.N. Sheremet, Mechanism of dislocation-governed charge transport in schottky diodes based on gallium nitride, Semiconductors 42 (2008) 689–693. https://doi.org/10.1134/S1063782608060092.
[34] J. Kotani, S. Tomabechi, T. Miyajima, N. Nakamura, T. Kikkawa, K. Watanabe, K. Imanishi, Tensile strain-induced formation of micro-cracks for AlGaN/GaN heterostructures, Phys. Status Solidi C 10 (2013) 808–811, https://doi.org/10.1002/pssc.201200627.
[35] P. Dalapati, S. Urata, T. Egawa, Investigation of AlGaN/GaN high electron mobility transistors on Silicon (111) substrates employing multi-stacked strained layer superlattice structures, Superlattice. Microst. 147 (2020) 106709, https://doi.org/10.1016/j.spmi.2020.106709.
[36] P. Narin, E. Kutlu-Narin, G. Atmaca, B. Sarikavak-Lisesivdin, S.B. Lisesivdin, E. Ozbay, A structural analysis of ultrathin barrier (In)AlN/GaN heterostructures for GaN-based high-frequency power electronics, Surf. Interface Anal. 54 (2022) 576–583, https://doi.org/10.1002/sia.7067.
[37] S. Besendörfer, E. Meissner, A. Lesnik, J. Friedrich, A. Dadgar, T. Erlbacher, Methodology for the investigation of threading dislocations as a source of vertical leakage in AlGaN/GaN-HEMT heterostructures for power devices, J. Appl. Phys. 125 (2019) 095704, https://doi.org/10.1063/1.5065442.
[38] J. Kotani, A. Yamada, T. Ishiguro, S. Tomabechi, N. Nakamura, Direct observation of nanometer-scale gate leakage paths in AlGaN/GaN and InAlN/AlN/GaN HEMT structures: Gate leakage paths in AlGaN/GaN and InAlN/AlN/GaN HEMT structures, Phys. Status Solidi A 213 (2016) 883–888, https://doi.org/10.1002/pssa.201532547.